

Towards Pattern-aware Data Augmentation for Temporal Knowledge Graph Completion

Jiasheng Zhang
University of Electronic Science and
Technology of China
Chengdu, China
zjss12358@std.uestc.edu.cn

Deqiang Ouyang
Chongqing University
Chongqing, China
deqiangouyang@cqu.edu.cn

Shuang Liang
Jie Shao
University of Electronic Science and
Technology of China
Chengdu, China
{shuangliang, shaojie}@uestc.edu.cn

ABSTRACT

Predicting missing facts for temporal knowledge graphs (TKGs) is a fundamental task, called temporal knowledge graph completion (TKGC). One key challenge in this task is the imbalance in data distribution, where facts are unevenly spread across entities and timestamps. This imbalance can lead to poor completion performance for long-tail entities and timestamps, and unstable training due to the introduction of false negative samples. Unfortunately, few previous studies have investigated how to mitigate these effects. Moreover, for the first time, we found that existing methods suffer from model preferences, revealing that entities with specific properties (e.g., recently active) are favored by different models. Such preferences will lead to error accumulation and further exacerbate the effects of imbalanced data distribution, but are overlooked by previous studies. To alleviate the impacts of imbalanced data and model preferences, we introduce *Booster*, the first data augmentation strategy for TKGs. The unique requirements here lie in generating new samples that fit the complex semantic and temporal patterns within TKGs, and identifying hard-learning samples specific to models. Therefore, we propose a hierarchical scoring algorithm based on triadic closures within TKGs. By incorporating both global semantic patterns and local time-aware structures, the algorithm enables pattern-aware validation for new samples. Meanwhile, we propose a two-stage training approach to identify samples that deviate from the model’s preferred patterns. With a well-designed frequency-based filtering strategy, this approach also helps to avoid the misleading of false negatives. Experiments justify that *Booster* can seamlessly adapt to existing TKGC models and achieve up to an 8.7% performance improvement.

PVLDB Reference Format:

Jiasheng Zhang, Deqiang Ouyang, Shuang Liang, and Jie Shao. Towards Pattern-aware Data Augmentation for Temporal Knowledge Graph Completion. PVLDB, 14(1): XXX-XXX, 2020.
doi:XX.XX/XXX.XX

PVLDB Artifact Availability:

The source code, data, and/or other artifacts have been made available at <https://github.com/zjs123/Booster>.

This work is licensed under the Creative Commons BY-NC-ND 4.0 International License. Visit <https://creativecommons.org/licenses/by-nc-nd/4.0/> to view a copy of this license. For any use beyond those covered by this license, obtain permission by emailing info@vldb.org. Copyright is held by the owner/author(s). Publication rights licensed to the VLDB Endowment.
Proceedings of the VLDB Endowment, Vol. 14, No. 1 ISSN 2150-8097.
doi:XX.XX/XXX.XX



Figure 1: An illustration of temporal knowledge graph.

1 INTRODUCTION

Temporal knowledge graphs (TKGs) are knowledge base systems that organize dynamic human knowledge in a structured manner. They are highly valuable for many applications such as event prediction [32] and recommendation systems [56]. As illustrated in Figure 1, a temporal knowledge graph is a dynamic directed graph characterized by node and edge categories, where nodes represent entities in the real world and labeled edges signify the relations between these entities. Each edge with its connected nodes can form a tuple (s, r, o, t) to describe a piece of dynamic knowledge (fact) in the real world, such as $(Messi, Transferto, PSG, 2021/11/8)$.

Due to delays in updates and limitations of extraction tools [27, 31, 57], TKGs are often incomplete, missing some facts existing in reality. To address this, predicting these missing facts—known as temporal knowledge graph completion (TKGC) [38]—has become a fundamental task to improve the quality of TKGs and support downstream tasks [13]. Several methods have been developed for TKGC, falling into two categories based on how they model temporal information: timestamp embedding models [7, 19, 46] that learn representation for each timestamp, and dynamic embedding models [12, 40, 45] that learn evolving entity and relation representations.

Despite their effectiveness, recent studies have shown that TKGs suffer from imbalanced data distribution [40], which may seriously impair the performance of TKG completion. Unfortunately, most existing methods overlook this aspect. They only report performance improvement on several metrics (e.g., mean reciprocal rank (MRR)) without thoroughly analyzing how the imbalanced data impacts their performance and how to alleviate such impacts, leading to less convincing and unsatisfactory results.

Previous limitations. The number of facts varies significantly across entities and timestamps. While a few have extensive fact descriptions, most only have a handful of related facts, resulting in imbalanced data distribution within TKGs. We first revisit the

completion performance of existing methods and find that they are severely affected by data imbalance in two key ways: **1) Unstable training.** Most existing methods are trained contrastively [41], treating facts existing in TKGs as positive and all others as negative. The models then learn to distinguish between these positive and negative samples. However, due to the imbalanced data distribution, many valid facts are missing in TKGs and mistakenly treated as negative samples (i.e., false negatives). This will mislead the training process and make the completion performance of entities with few facts deteriorate during training. **2) Imbalanced performance.** The uneven distribution of facts across timestamps causes the performance of existing methods to vary dramatically depending on the timestamp, even between adjacent timestamps. The neglect of uneven distribution makes the training process of these methods further aggravate such performance imbalance (Section 3.3).

While examining the effects of imbalanced data distribution, we further identified a previously unrecognized problem: existing methods also exhibit a **model preference issue** that can worsen the impact of data imbalance. During completion, existing methods favor entities with specific properties according to their architectures (Section 3.4). For example, tensor factorization-based models [19] prioritize frequently interacted entities, whereas recurrent neural network-based models [40] favor recently active entities. Such preferences can make it difficult for these models to learn TKG patterns that deviate from the model’s preferences, especially when valid samples fitting these patterns are mistakenly treated as false negatives.

Technical challenges. Although some data augmentation approaches have been proposed to solve similar imbalanced data issues for general graphs and static knowledge graphs [8, 26, 34], they face key challenges when applied to TKGs: **1) False negative filtering.** Some of these methods simply filter neighboring nodes as false negatives [55]. They cannot consider various components (i.e., entities, relations, and timestamps) within TKGs’ complex graph structure, failing to achieve adequate filtering. **2) New samples generation.** They generate new samples solely based on node connectivity. However, TKGs have intricate semantic and temporal patterns brought by diverse entity and relation categories, as well as time-evolving topology. New samples must therefore fit with these patterns. **3) Training procedure.** Most of them simply train the models on the refined graph data without considering model preference issues, leading to low generalization to various TKG patterns.

The proposed work. We present *Booster*, the first pattern-aware data augmentation strategy specialized to TKGs to tackle their imbalanced data and model preference issues. It uses three frequency-based filtering strategies tailored to different components of TKGs, considering both intra-component and inter-component interaction frequencies to adequately filter potential false negatives. A hierarchical scoring algorithm then classifies these samples as either hard negatives or false negatives, ensuring the identified false negatives fit both the global semantic patterns shared across all facts and the recent trends within the local graph structure, which can be used to enrich the imbalanced data. Finally, a two-stage training approach is proposed. The models are first pre-trained on filtered high-quality facts to avoid the misleading of false negatives and identify preference-deviated facts, and then fine-tuned on hard

negatives, false negatives, and preference-deviated facts to inject pattern-aware fine-grained information while enhancing pattern generalization ability. Experiments on 5 real-world TKGs show that *Booster* can seamlessly adapt to existing TKGC methods, improving their performance up to 8.7%, surpassing typical temporal graph and knowledge graph data augmentation techniques on average of 7.1%, while also reducing performance variance of existing TKGC models by 22.8% on average. Our contributions are as follows:

- We make the first attempt to investigate the imbalanced data and model preference issues of TKG completions.
- We propose the first pattern-aware data augmentation strategy tailored to TKGs—*Booster*, which can generate new samples fitting TKG patterns and enhance the model’s generalization ability to different patterns.
- Experimental results show that *Booster* can effectively improve the performance of existing TKGC models.

2 RELATED WORK

2.1 Temporal Knowledge Graph Completion

Temporal knowledge graph completion aims to predict missing facts based on observed ones within TKGs. Existing methods can be divided into two categories: 1) Timestamp embedding methods [19, 48, 51] that learn representations respectively for entities, relations, and timestamps, and use these embeddings to predict the missing facts. For example, HyTE [7] integrates the learnable timestamp embeddings into the translation function of the TransE model [1]. TNT [19] uses 4-order tensor factorization to generate these embeddings. On this basis, Timeplex [16] extends by considering the recurrent nature of relations, while TELM [44] extends by learning multi-vector representations with canonical decomposition. Recently, QDN [36] uses a quadruplet distributor network to support the fourth-order factorization. MADE [37] proposes to learn multi-curvature representations. 2) Dynamic embedding methods [7, 15, 46, 52] that learn time-evolving entity and relation representations to model their changing semantics. DE [12] uses nonlinear operations to model various evolution trends of entity semantics. TA [10] utilizes a sequence model to generate time-specific relation representations. CENET [47] employs historical contrastive learning to learn temporal dependencies. Recently, some studies have attempted to model structure information of TKGs via graph neural networks [11]. For example, TEMP [40] uses self-attention to model the spatial and temporal locality. RE-GCN [21] auto-regressively models historical sequence. LogCL [4] learns both local and global historical structures.

Despite their effectiveness, unfortunately, none of them deeply investigated the imbalanced data distribution issue [40] inherent in the TKGs. Neither how imbalanced data affect their completion performance, nor how to alleviate such impacts are studied, making their results less convincing and unsatisfactory. A recent work, TILP [43], claims that its logic rule-based method is less affected by imbalance. However, its strategy lacks the adaptability to other TKGC models.

2.2 Graph Data Augmentation

Some data augmentation strategies have been developed recently to improve the data quality for graphs [6, 14, 23, 26, 53], which

helps to reduce the effects of imbalanced data distributions in general graph modeling (e.g., degree bias [33]). For example, AIA [30] adversarially generates masks on graphs to handle distribution shift. GraphPatcher [17] generates virtual nodes for ego-graphs to mitigate the degree bias. Recently, some studies have also explored the data augmentation strategies for temporal graphs [35]. For example, MeTA [39] modifies temporal topology and features to enhance model robustness. TGEitor [54] conducts task-guided graph editing for temporal transaction networks. However, these strategies are designed for general graphs without considering complex semantics brought by node and edge categories, and thus fail to generate samples that fit TKG patterns.

Recently, the issue of imbalanced data in static knowledge graphs has also gained increasing attention. Some studies develop advanced negative sampling strategies to avoid false negatives [18, 25, 49]. For example, NSCaching [55] uses an importance sampling approach to adaptively identify high-quality negative samples. DeMix [5] introduces a self-supervised mechanism to identify negative samples. However, these strategies encounter challenges when applied to TKGs, as they fail to consider the temporality of facts. Moreover, these methods often rely on path searching or adversarial training, which can be highly time-consuming for TKGs with lengthy historical sequences. Some researches also investigate to generate new facts to enrich the imbalanced data [26, 34, 50]. For example, KG-Mixup [28] generates synthetic facts in the embedding space to mitigate degree bias. KGCF [3] augments with counterfactual relations. However, they can neither generate new facts that fit the complex semantic and temporal patterns within TKGs, nor do they address model preference issues.

Overall, although data augmentation has been widely studied to address data imbalance for general graph learning, it remains an unexplored area for TKGs. Existing data augmentation strategies either face high time-consuming for TKGs with lengthy historical sequences, or are unaware of complex semantic and temporal patterns within TKGs, leading to an urgent for a data augmentation strategy specialized to TKGs.

3 PRELIMINARY STUDY

3.1 Temporal Knowledge Graph

A temporal knowledge graph is denoted as $\mathcal{G} = (\mathcal{E}, \mathcal{R}, \mathcal{T}, \mathcal{F})$. \mathcal{E} and \mathcal{R} are entity set and relation set, respectively. \mathcal{T} is the set of observed timestamps and \mathcal{F} is the set of facts. Each tuple $(s, r, o, t) \in \mathcal{F}$ connects the subject and object entities $s, o \in \mathcal{E}$ via a relation $r \in \mathcal{R}$ in timestamp $t \in \mathcal{T}$, which means a unit knowledge (i.e., a fact).

3.2 Temporal Knowledge Graph Completion

Temporal knowledge graph completion aims to predict the missing facts through the existing ones. Given an incomplete fact $(s, r, ?, t)$, the task identifies the most likely object entity o_c from the candidate set \mathcal{E} . Each candidate fact (s, r, o_c, t) is ranked by confidence score, and the highest-ranking candidate is chosen as the new fact. The rank of the true object entity, denoted as $rank(s, r, o, t)$, is the basic metric of this task (lower is better). It indicates the position of the correct object entity o among all candidate entities $o_c \in \mathcal{E}$. Building on this, mean reciprocal rank (MRR) is calculated as the average

reciprocal rank across all facts, defined as:

$$MRR = \frac{1}{|Test|} \sum_{(s,r,o,t) \in Test} \frac{1}{rank(s,r,o,t)}. \quad (1)$$

A higher MRR value indicates better model performance.

3.3 Imbalanced Data Distribution

In this part, we selected three typical TKG methods (i.e., DE [12], TNT [19], and TEMP [40]) to evaluate their completion performance on the most popular TKG dataset ICEWS14 [2]. Our results demonstrate issues with unstable training and inconsistent performance. Further analysis shows that these limitations stem from the imbalanced data distribution within TKGs, which for the first time reveals the impacts of imbalanced data distribution on existing TKG methods.

Unstable training. As shown in Figure 2(a), existing methods suffer from unstable training in two aspects: 1) The effectiveness of training is inconsistent across different samples. The *rank* metrics of some facts may gradually increase during training (e.g., sample 1 in the TNT model), showing that training can unintentionally damage their completion performance. Meanwhile, the *rank* metrics for some facts can only fluctuate near a large number (e.g., sample 2 in the DE model), indicating that training cannot effectively optimize their completion performance. 2) The effectiveness of training is inconsistent across different runs. In the DE model, sample 1 shows highly inconsistent performance across four independent training runs. The fluctuation range of the *rank* metric widens as the training progresses, indicating that the inconsistency becomes more serious.

To study the cause of the unstable training, we split the facts into different sets based on the fluctuation range of the *rank* metric across four independent runs, and then calculate the average degree for entities involved in each set. As shown in Figure 2(b), we can see that as the average degree decreases, both the fluctuation range and the average *rank* increase, highlighting that unstable training is more likely to occur for entities with sparse local structures. This is because existing methods typically focus on distinguishing between positive and negative samples, treating facts in TKGs as positive and all others as negative. However, entities with sparse local structures often have missing yet valid facts, introducing many false negative samples that will mislead the training [55].

Imbalanced performance. As shown in Figure 2(c), existing methods suffer from imbalanced performance: 1) MRR varies significantly across different timestamps, with considerable gaps even between adjacent timestamps. 2) The performance can be notably poor for some timestamps. 3) As training progresses, the standard deviation of MRR will increase, suggesting that the performance imbalance of existing methods may worsen over training. To investigate the cause of imbalanced performance, as shown in Figure 2(d), we calculate the average degree and the average MRR for each timestamp. We can see that there exists a synchronization between the fluctuation trends of the average degree and MRR, with their peaks and troughs occurring simultaneously, albeit with some displacement and scaling. This finding suggests that an imbalanced data distribution across timestamps can lead to performance imbalance for existing TKG methods.

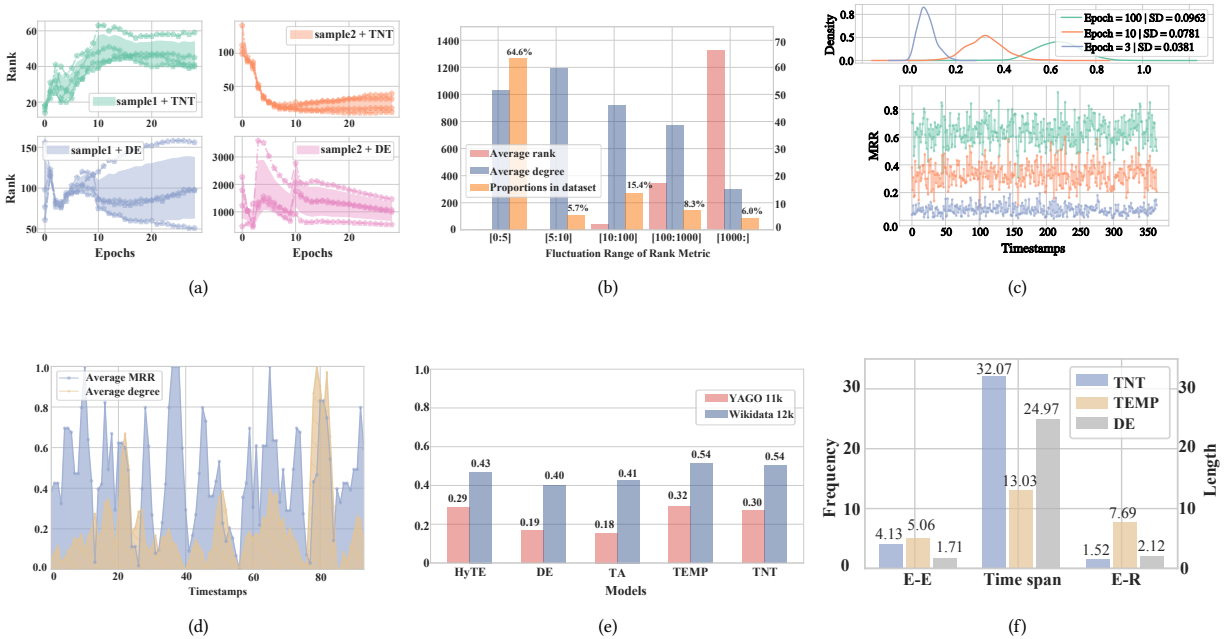


Figure 2: (a) Change of the *rank* metric during training. Each training is independently repeated four times and the color-filled part is the fluctuation range of the *rank* metric across four training runs. (b) The average degree of samples with different *rank* fluctuation ranges. (c) MRR of the TEMP model across different timestamps. The top plot displays the density function of the MRR distribution at different epochs. SD refers to standard deviation. (d) MRR and the average degree of entities in different timestamps. (e) Proportions of positive samples among the top-10 ranked candidates for different models. (f) The statistical characteristics of the top-ranked entities for different models.

These observations suggest that current TKGC methods face significant challenges due to unstable training and imbalanced performance stemming from imbalanced data distribution. Addressing these issues is crucial to improving their effectiveness.

3.4 Model Preference

Some studies use self-training to address data imbalance, selecting high-scoring unlabeled samples as pseudo-positive samples and adding them to the training data [22]. However, does this strategy also work for temporal knowledge graph completion models? As shown in Figure 2(e), the top-ranked samples of existing TKGC models are not always positive (e.g., only 30% of top-10 ranked samples by TNT are positive), indicating that using self-learning for these TKGC models will introduce a large number of noisy samples. Although reducing the size of pseudo-positive samples can help mitigate such noise, the challenging issue of model preference continues to hinder self-training in TKGC models—an aspect overlooked in previous research.

As shown in Figure 2(f), we analyze the data properties of the top-ranked entities from different models. “E-E” means the frequency of the candidate entity interacting with other entities. “Time span” means the length between the test timestamp and the candidate entity’s nearest active timestamp. “E-R” means the frequency of the candidate entity interacting with the relation in the query. We can

see that the top-ranked entities from different models have significant differences in their data properties. For example, TNT prefers frequently interacted entities, while TEMP prefers recently active entities and entities that have interactions with the query relation, revealing that existing TKGC methods suffer from **model preference** that they prefer entities with specific properties. Previous studies have shown that facts in TKGs often follow diverse patterns [42]. However, the model preference issue makes TKGC models struggle to learn facts that deviate from their favored patterns (especially when they are mistakenly treated as false negatives). This challenge becomes even more serious with self-training, as the model consistently selects samples with one pattern as new training data, which degrades the model’s generalization ability to other TKG patterns.

These observations show that current TKGC methods suffer from model preferences, limiting the effectiveness of traditional data augmentation strategies (e.g., self-training). Unfortunately, no previous work has investigated how to address this challenge.

4 METHOD

4.1 Overall Architecture

Our above discussions emphasize the urgent need for a data augmentation strategy tailored to TKGs, enriching imbalanced data distribution, and alleviating misleading from false negatives and

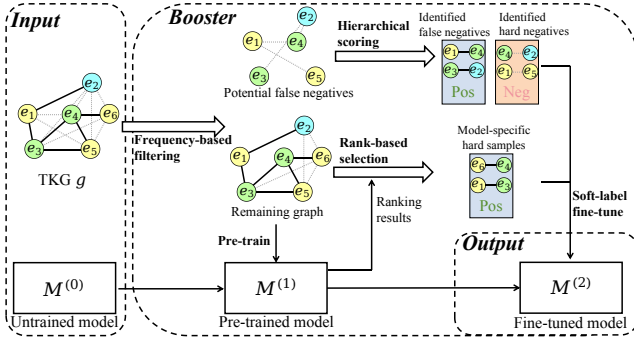


Figure 3: The conceptual illustration of the overall architecture of *Booster*, where the black solid lines indicate the observed facts in TKG and the gray dashed lines indicate facts do not exist in TKG. We hide the time annotations and edge types in the figure for brevity.

model preferences. To this end, we introduce *Booster*, a data augmentation framework that can generate pattern-aware new samples to enrich TKG structure and reduce misleading through a two-stage training approach.

As shown in Figure 3, *Booster* takes a TKG \mathcal{G} and an untrained TKG model $M^{(0)}$ as input. In the first stage, it uses a frequency-based filtering strategy to filter out potential false negatives, and then pre-trains $M^{(0)}$ on the remaining data. This step serves a main purpose: protecting the model from misleading false negatives, and thus enabling accurate selection of preference-deviated samples. Low-ranked positive samples reveal which facts the model is hard to learn (i.e., those it does not prefer).

In the second stage, a hierarchical scoring algorithm is used to further separate potential false negatives into real false negatives and hard negatives. The pre-trained model $M^{(1)}$ is then fine-tuned on these identified samples, along with preference-deviated facts, to produce the final model $M^{(2)}$. This process has two key benefits: 1) enriching sparse data by incorporating validated false negatives as additional positive samples, and 2) emphasizing hard samples unique to the data and model to reduce misleading stemming from data imbalances and model preferences. Notably, *Booster* is plug-and-play and compatible with any existing TKG model.

4.2 Frequency-based Filtering

Compared with general graph data, filtering potential false negatives for TKGs faces several unique challenges: 1) TKGs contain various components (i.e., entities, relations, and timestamps). The co-occurring patterns within TKGs often involve several different components, requiring the filtering strategy to fully consider these intra- and inter-component patterns. 2) The integration of time annotations results in a long historical graph sequence and multiple edges between nodes, requiring the filtering strategy to consider the distribution of these edges in the time dimension. Therefore, we propose a frequency-based filtering approach, using tailored strategies for each component to filter false negatives effectively.

Relation-based filtering. Relations in TKGs have significant co-occurring patterns [56]. For example, “economic sanctions” and “export restriction” are a pair of relations that often co-occur between two hostile countries. After the relation “transfer to” occurs between a player and a football club, the relation “play for” will subsequently occur between them. This inspires us that edges missing in a TKG but fitting these relation patterns are likely to be false negatives, and we can detect them by identifying these patterns. Therefore, for each relation r we construct its co-occurred relation set as $R(r) = \{r_i | (s_j, r, o_j, t_j) \in \mathcal{G}, (s_j, r_i, o_j, t'_j) \in \mathcal{G}, |t_j - t'_j| < L_r\}$ where L_r is a hyper-parameter. Then, for each observed fact $(s, r, o, t) \in \mathcal{G}$ we can filter its corresponding potential false negatives as $(s, r_i, o, t) \notin \mathcal{G}$ where $r_i \in R(r)$. We further refine the filtering by considering the inter-component patterns and pattern frequencies. First, entities have preferences to interact with a specific set of relations (e.g., athletes are more likely to have relation “play for”), so recognizing these entity-relation interaction patterns helps exclude unrealistic combinations. Second, the higher frequency of relations within $R(r)$ indicates a more important pattern. By retaining only the top- m most frequently co-occurring relations in $R(r)$, we can filter out low-confidence patterns, reduce potential false negatives, and thus lower the time required for scoring in the next step. Therefore, we filter out the relation-based false negatives for each fact $(s, r, o, t) \in \mathcal{G}$ as:

$$RN_{(s,r,o,t)} = \{(s, r', o, t) | r' \in \tilde{R}(r) \cap \tilde{R}(s), (s, r', o, t) \notin \mathcal{G}\}, \quad (2)$$

where $\tilde{R}(r)$ is the subset of $R(r)$ which only preserves top- m most frequent relations. Similarly, $\tilde{R}(s)$ is the frequency filtered subset of $R(s) = \{r_k | (s, r_k, o_k, t_k) \in \mathcal{G}\}$, which preserves top- m frequently interacted relations of entity s .

Entity-based filtering. While the above strategy filters false negatives based on relation semantics, the connectivity among entities also provides insights into the occurrence of facts. Entities often have preferences to interact with a specific set of entities (e.g., “Israel” and “Houthis in Yemen” frequently interact due to ongoing conflict), inspiring us that facts fitting entity co-occurring patterns but missing in \mathcal{G} are likely to be false negatives. Therefore, for each entity e we construct its co-occurring entity set as $N(e) = \{e_i | (e, r_i, e_i, t_i) \in \mathcal{G}\}$, and filter the corresponding top- m frequency entities as $\tilde{N}(e)$. Subsequently, we filter out the entity-based false negatives for each fact $(s, r, o, t) \in \mathcal{G}$ as:

$$EN_{(s,r,o,t)} = \{(s, r, o', t) | o' \in \tilde{N}(s), r \in \tilde{R}(o'), (s, r, o', t) \notin \mathcal{G}\}, \quad (3)$$

indicating entity pairs that are likely to connect through the relation r but are missing in TKG. This is achieved by filtering the entity o' that frequently interacts with s (i.e., $o' \in \tilde{N}(s)$), and has prior interactions with relation r (i.e., $r \in \tilde{R}(o')$).

Time-based filtering. Some facts may be repeated many times over a short period, such as “(Region A, Armed attack, Region B)” or “(Country A, Hold negotiations with, Country B)”. Due to the limitation of the update frequency of TKGs, repeated facts may be missing in some timestamps. Therefore, we can detect potential false negatives by finding the omissive timestamp within the time interval where the fact repeats. Specifically, we filter out the time-based false negatives for each fact $(s, r, o, t) \in \mathcal{G}$ as:

$$TN_{(s,r,o,t)} = \{(s, r, o, t') | t' \in [x, t], (s, r, o, x) \in \mathcal{G}, (s, r, o, t') \notin \mathcal{G}\}. \quad (4)$$

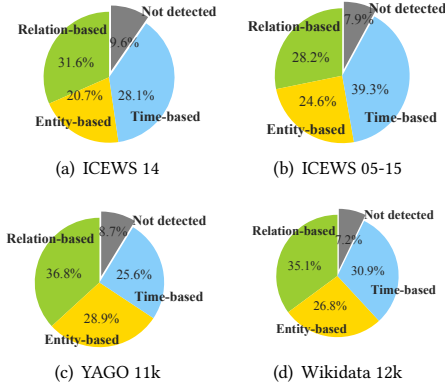


Figure 4: The proportion of false negative samples detected by the frequency-based filtering strategy in four real-world datasets.

Notably, we restrict that $t - x < L_t$ to ensure only focusing on short-period repetitions, where $t - x$ indicates the fact repetition period and L_t is a hyper-parameter with a small value.

We only perform these filtering strategies for observed facts with sparse local structures (i.e., $N(s) \leq k$ or $N(o) \leq k$) to reduce the time complexity. To verify the effectiveness of our strategies, we randomly remove 20% facts from \mathcal{G} and calculate how many of them can be detected by our strategies. As shown in Figure 4, more than 90% of removed facts can be detected, highlighting the effectiveness of our strategy in filtering potential false negatives.

Filtering out these potential false negatives can prevent the model from being misled and enrich the sparse structure by further identifying real false negatives. Moreover, since these strategies have considered intrinsic patterns of TKG, the filtered samples contain fine-grained information that enhances the model’s ability when used for fine-tuning.

4.3 Hierarchical Scoring Algorithm

Identifying real false negatives is challenging, for two reasons. 1) TKGs have intricate semantic and temporal patterns brought by diverse entity and relation categories, as well as time-evolving topology. To accurately recognize real false negatives, it is essential to account for these patterns adequately. 2) TKGs are usually incomplete with noise graph structures, making the identification inevitably have some mistakes. Thus, it is crucial to assess the confidence of each fact to prevent the model from being misled by low-confidence false negatives.

In this part, we propose a novel hierarchical scoring algorithm, assigning scores for potential false negatives to indicate their possibility to be real false negatives. To incorporate both the local structures and the global patterns of TKG while alleviating the effect of skewed data distribution, our algorithm divides the scoring process into two parts: global pattern counting and local structure aggregation. As shown in Figure 5, the former generates global scores via counting triangles on the unified graph, and the latter aggregates the global score based on the local structure of a sample. It uses a hierarchical structure (i.e., entity scores and relation scores)

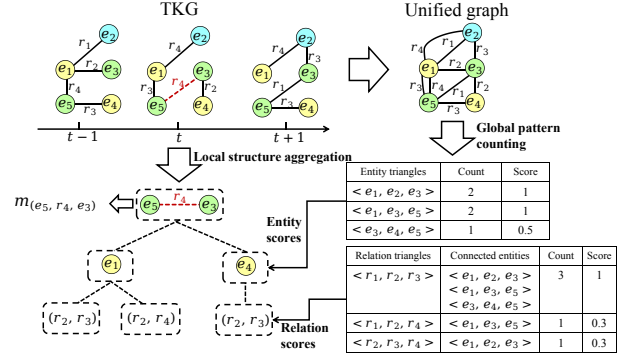


Figure 5: An example of the hierarchical scoring algorithm, where the red dashed line denotes the potential false negative fact that needs identification.

to alleviate the complexity explosion brought by combinations of node and edge categories. Additionally, a perturbation technique is used to estimate the stabilization of the scoring process, reducing the impact of noisy graph structures.

Global pattern counting. We represent the semantic patterns of TKGs as triangle closures that include node and edge categories. By identifying frequent triangles and estimating their intensity (i.e., the likelihood that a third edge will complete the triangle when two edges are present), we can effectively capture and quantify these patterns. However, directly counting triangles in TKGs yields a vast number of distinct triangles due to the mix of various entities, relation types, and temporal orders, making the process time-consuming and leading to sparse counts that poorly reflect triangle intensity. To address this, we propose decomposing entities and relations within triangles to reduce the complexity and using a time-irrelevant graph to reduce noise from temporal ordering.

The time-irrelevant graph contains all the entity-relation-entity combinations observed in TKG, represented as $\mathcal{G}' = \{(s, r, o) | (s, r, o, t) \in \mathcal{G}\}$. Since \mathcal{G}' has been removed from the non-uniform distribution of data in the time dimension, it can faithfully reflect the preferences among entities and relations. To alleviate the complexity explosion brought by the combination of entity and relation types in triangle counting, we first anonymize the relation types in \mathcal{G}' to count entity triangles. We define the number of edges between entities as $N(e_1, e_2) = |\{(e_1, r, e_2) | (e_1, r, e_2) \in \mathcal{G}'\}|$ where $|\cdot|$ means the size of the set. The number of triangles among entities can be consequently defined as:

$$C_e(e_1, e_2, e_3) = \min(N(e_1, e_2), N(e_2, e_3), N(e_1, e_3)), \quad (5)$$

which counts for the number of edges existing among three entities. Since the anonymization of relation types highlights the connectivity of the graph, C_e can accurately reflect the connection preference among entities, e.g., China and Japan have more connections with South Korea than the Vatican. Finally, we obtain the entity score by normalization as:

$$S_e(e_1, e_2, e_3) = \frac{C_e(e_1, e_2, e_3) - \min(C_e) + 1}{\max(C_e) - \min(C_e) + 1}, \quad (6)$$

where $\max(C_e)$ and $\min(C_e)$ are respectively the maximum number and minimum number of entity triangles in \mathcal{G}' .

The relation triangles indicate the interaction rules among entities (e.g., the combination of relations “launching an attack”, “call for support”, and “impose sanctions” describes the hostile behavior among three countries), and thus are important to identify the missing valid facts. This motivates us to anonymize the entities in \mathcal{G}' to find relation triangles. Specifically, a relation triangle consists of three relations that connect the entities within an entity triangle. We define the count of each relation triangle as how many different entity triangles are connected by it, which is formally defined as:

$$C_r(r_1, r_2, r_3) = |\{(e_i, e_j, e_k) | (e_i, r_1, e_j), (e_j, r_2, e_k), (e_i, r_3, e_k) \in \mathcal{G}'\}|. \quad (7)$$

The same normalization is then employed on C_r to obtain the relation score S_r . In summary, a high entity score suggests that three entities are more likely to form a triangle, while a high relation score indicates a stronger connection among the entities through three specific relations. This effectively quantifies the patterns present in the TKG.

Local structure aggregation. The validity of a fact depends not only on its alignment with global semantic patterns but also on its relevance to recent facts. While global scores summarize the semantic patterns within TKGs, we propose aggregating them based on the local structure of each fact to consider its short-term relevance. As shown in Figure 5, we reformulate the local structure of each potential false negative fact (s, r, o, t) into an entity layer and a relation layer, allowing us to hierarchically aggregate the global scores. The entity layer contains all entities that have interactions with both s and o within the time window L_e , denoted as $l_e(s, o, t)$. Therefore, each entity e in the entity layer can form a triangle with s and o , allowing us to estimate the validity of (s, r, o, t) based on intensities of entity triangles (i.e., the likelihood that $s - o$ will exist when $s - e$ and $o - e$ are present). To integrate relation scores, for each entity $e \in l_e(s, o, t)$, we construct its corresponding relation layer $l_r(s, o, t, e)$. Each item in relation layer is represented as (r_i, r_j) , where r_i are relations existing between s and e within L_e , and r_j are relations existing between o and e within L_e . Therefore, each item (r_i, r_j) in the relation layer can form a triangle with r , allowing us to estimate the validity of (s, r, o, t) based on intensities of relations triangles (i.e., the probability that s and o are connected by r given that s and o have connected with e through r_i and r_j). Afterward, we aggregate the relation layer as:

$$m_{e_i} = \sum_{(r_i, r_j) \in l_r(s, o, t, e_i)} \alpha_{i,j} \cdot S_r(r_i, r_j, r), \quad (8)$$

where $e_i \in E(s, o, t)$ represents each node in the entity layer of (s, r, o, t) . We use α as a time-aware weight to emphasize facts that occurred more recently, which is defined as:

$$\alpha_{i,j} = \text{softmax}(-|t_i - t_j|), \quad (9)$$

where t_i and t_j are respectively the occurring time of facts (s, r_i, e) and (e, r_j, o) . We then aggregate the entity layer as:

$$m_{(s,r,o,t)} = \sum_{e_i \in E(s,o,t)} m_{e_i} \cdot (1 + S_e(s, o, e_i)), \quad (10)$$

where $m_{(s,r,o,t)}$ is the confidence score of (s, r, o, t) .

Score perturbation. Each potential false negative fact originates from an observed fact (see Section 4.2), sharing a similar local structure. Therefore, we can achieve the adaptive threshold

by comparing their scores. A potential false negative f' will be identified as a real false negative if $m_{f'} > m_f$ where f is its corresponding observed fact. However, the scoring process inevitably has noise because of the incomplete graph structure. We extend our algorithm with the perturbation technique and smooth labels. For each potential false negative f' , we first slightly perturb its corresponding hierarchical structures (e.g., randomly repeat or remove items within layers or perturb the time-aware weights), and then calculate a set of scores $M_{f'} = \{m_{f'}^1, m_{f'}^2, \dots, m_{f'}^k\}$ based on these perturbed hierarchical structures. If $\text{mean}(M_{f'}) > m_f$, we will set $\text{mean}(M_{f'})$ as a smooth label for f' , which emphasizes the samples with more robust structures and more stable patterns. The remaining facts are regarded as hard negative samples.

Notably, although data-driven methods can also be trained to identify false negative facts, such as HyTE [7] and DE [12], our algorithm has three main advantages. First, our algorithm can generate reliable confidence scores for these facts, providing more fine-grained information. Second, our algorithm requires no additional training and thus is more efficient. Third, our algorithm considers various patterns within TKG, helping in achieving more accurate identification. Although some data-driven methods also consider patterns, they typically involve complex architectures that demand extensive training time.

4.4 Two-Stage Training

The filtering strategies can identify potential false negatives, while the hierarchical scoring algorithm further distinguishes between real false negatives and hard negatives. On this basis, we propose a two-stage training approach to shield the model from imbalanced data and alleviate the model preferences.

Pre-training. Our filtering strategies have identified potential false negatives that may be valid facts but are missing in a TKG. To avoid misleading, we exclude these from being used as negative samples during contrastive training. Formally, given an untrained TKGC model $M^{(0)}$, we pre-train it using

$$L_p = \sum_{(s,r,o,t) \in \mathcal{G}} -\log\left(\frac{\exp(p(s,r,o,t))}{\sum_{Neg(s,r,o,t)} \exp(p(s,r,e,t))}\right) + \lambda, \quad (11)$$

where each $Neg(s, r, o, t)$ are filtered negative facts specific to $((s, r, o, t))$, defined as $Neg(s, r, o, t) = \{(s, r, e, t) | e \in \mathcal{E}, (s, r, e, t) \notin EN_{(s,r,o,t)} \cup RN_{(s,r,o,t)} \cup TN_{(s,r,o,t)}\}$. λ is a regularization term and $p(\cdot)$ is the prediction score obtained by model $M^{(0)}$. The pre-trained model is denoted as $M^{(1)}$.

Since the pre-training process avoids the misleading effects of false negatives, the lower-ranked positive samples from the pre-trained model $M^{(1)}$ accurately reveal which facts the model is hard to learn (i.e., whose pattern it does not prefer), and thus indicate model preferences. We select these low-ranked positive samples as model-specific hard samples, emphasizing them during training to correct misleading introduced by the model preferences. Formally, for each positive sample $(s, r, o, t) \in \mathcal{G}$ with its corresponding negative samples $(s, r, e, t) \in Neg(s, r, o, t)$, we select (s, r, o, t) as a model-specific hard sample if it is not ranked higher than all of (s, r, e, t) by $M^{(1)}$. We denote the model-specific hard samples as \mathcal{F}_m and use them for fine-tuning.

Fine-tuning. We then fine-tune the model $M^{(1)}$ on the identified real false negatives, hard negative samples, and the model-specific hard samples to obtain the final model $M^{(2)}$. This has three key purposes: 1) During fine-tuning, real false negatives are treated as positive samples, helping to enrich the data for entities and timestamps with sparse local structures. This approach reduces the performance imbalance caused by uneven data distribution. Meanwhile, the smooth labels generated through the perturbation strategy emphasize facts with more robust structures and more stable patterns, providing TKGC models with finer-grained information. 2) Hard negative samples are facts that resemble positive samples in pattern but are actually invalid, making them difficult for the model to distinguish. Fine-tuning on these samples enhances the model’s discrimination ability. 3) Model-specific hard samples reflect patterns that the model is hard to learn. Therefore, fine-tuning on them can force the model to adapt to these non-preferred patterns, enhancing the model’s generalization ability to various TKG patterns. Formally, we fine-tune the pre-trained model $M^{(1)}$ using

$$L_f = \sum_{f \in \mathcal{G}^P} -l_f \log \sigma(p(f)) + \sum_{f' \in \mathcal{G}^n} -\log \sigma(p(f')), \quad (12)$$

where \mathcal{G}^P contains real false negatives and model-specific hard samples, while \mathcal{G}^n contains hard negative samples. $\sigma(\cdot)$ is the sigmoid function and $l_f = \text{mean}(M_f)$ is the smooth label of fact f . The fine-tuned model $M^{(2)}$ thus has eliminated the effects of imbalanced data and model preferences.

4.5 Complexity Analysis

The additional time complexity introduced by *Booster* comes from the filtering strategy and the hierarchical scoring algorithm. During filtering potential false negatives, for each observed fact, it takes $O(n_r)$ time to achieve the relation-based filtering, where n_r is the number of relations that co-occur with relation r . The time for entity-based filtering is $O(n_{s,o})$ where $n_{s,o}$ is the number of entities that have interacted with entities s and o , and the time for time-based filtering is $O(L_t)$. For the hierarchical scoring, by iterating over the unified graph, the time for calculating the entity score and relation score is $O(|\mathcal{E}|^2)$ where $|\mathcal{E}|$ is the number of entities within TKG. During local structure aggregation, it takes $O(n_{s,o} \cdot q_{s,e} \cdot q_{o,e})$ time for each sample where $q_{s,e}$ is the number of relations between s and the co-interacted entity e .

5 EXPERIMENTS

We conduct experiments on five benchmark datasets to answer the following research questions: **RQ1**: Can *Booster* improve the performance of existing models? **RQ2**: How does each component of *Booster* contribute to performance improvement? **RQ3**: Is *Booster* efficient? **RQ4**: Can *Booster* improve the balance and stabilization of the performance?

Datasets. We evaluate *Booster* on five benchmark TKG datasets, which are from ICEWS [2], YAGO [29], Wikidata [9], and GDEL T [20]. ICEWS contains interactions among political people and countries with time annotations. We use two subsets of it, i.e., ICEWS 14 and ICEWS 05-15, which contain knowledge in 2014 and knowledge

Table 1: Statistics of datasets.

Dataset	$ \mathcal{E} $	$ \mathcal{R} $	$ \mathcal{T} $	$ \mathcal{F} $
ICEWS 14	7,128	230	365	90,730
ICEWS 05-15	10,488	251	4,017	461,329
YAGO 11k	10,623	10	2,801	20,507
Wikidata 12k	12,554	24	2,270	40,621
GDEL T	500	20	366	3,419,607

from 2005 to 2015 respectively. YAGO is a knowledge base that contains common sense knowledge. YAGO 11k is formed by selecting knowledge that contains the top-10 frequent time-sensitive relations from YAGO. Wikidata is an open knowledge base driven from Wikipedia and Wikidata 12k is a subset of it. GDEL T is a large political knowledge base. We split each dataset as train/validation/test set with the proportion of 8:1:1. The detailed statistics of these datasets are shown in Table 1.

Comparison models. We compare *Booster* with existing data augmentation strategies for temporal graphs (MeTA [39]) and knowledge graphs (DeMix [5], NSCaching [55], and KG-Mixup [28]). We use five popular TKGC models as backbones to evaluate the effectiveness of these data augmentation strategies: HyTE [7], TA [10], DE [12], TNT [19], and TEMP [40].

Implementation details. We use the released official implementation of existing TKGC models as the backbone. For each model, we tune its hyper-parameters using a grid search, where the best hyper-parameter settings are selected with the best MRR on the validation set. We create 100 mini-batches for each epoch during training, and the number of epochs is set as 1000. The models are pre-trained in the first 20 epochs and then fine-tuned in the rest epochs with early stopping. The learning rate is set as 0.001. For all models, we set the representation dimension d as 200, the size of negative sampling as 50, and the data pre-processing is unified as in TNT [19] to achieve fair comparison. The time windows L_r , L_e , and L_t are selected from $\{1, 3, 5, 10, 20\}$. We use Adagrad [24] for optimization and all experiments are conducted on a 64-bit machine with Nvidia TITAN RTX. Besides MRR, we also use Hits@k as the metric which is defined as $\text{Hits}@k = \frac{1}{|\mathcal{T}_{est}|} \sum_{(s,r,o,t) \in \mathcal{T}_{est}} \text{ind}(\text{rank}(s, r, o, t) \leq k)$, where $\text{ind}()$ is 1 if the inequality holds and 0 otherwise. Our source code is available at <https://github.com/zjs123/Booster>.

5.1 Overall Evaluation (RQ1)

Accuracy. Table 2 shows the performance of existing TKGC models with different data augmentation strategies. We can see that: (1) *Booster* can bring performance improvements for all backbone models. The maximum improvement is 8.7% and the average improvement is 4.5% with statistical significance, demonstrating that *Booster* can seamlessly adapt to existing models to improve the quality of the learned representations. The HyTE model gets the largest improvement (8.7% in MRR on the ICEWS 14 dataset and 7.9% in MRR on the ICEWS 05-15 dataset). This is because HyTE independently learns representations in different timestamps and thus is more sensitive to the imbalanced data distribution. *Booster* can enrich the sparse structure by identifying false negatives and thus achieve improvement. (2) Compared with existing graph data augmentation strategies, *Booster* can achieve higher performance

Table 2: Performance comparison of baseline models. The best results are boldfaced and “DA” means data augmentation.

TKGC models	Dataset DA strategies	ICEWS 14			ICEWS 05-15			YAGO 11k			Wikidata 12k		
		MRR	Hits@1	Hits@3	MRR	Hits@1	Hits@3	MRR	Hits@1	Hits@3	MRR	Hits@1	Hits@3
HyTE	Without DA	0.297	0.108	0.416	0.316	0.116	0.445	0.134	0.032	0.181	0.191	0.107	0.208
	MeTA	0.293	0.105	0.410	0.319	0.117	0.449	0.132	0.031	0.178	0.186	0.105	0.201
	DeMix	0.301	0.113	0.412	0.323	0.126	0.447	0.136	0.035	0.182	0.193	0.108	0.211
	NSCaching	0.295	0.107	0.414	0.320	0.124	0.445	0.130	0.029	0.179	0.188	0.105	0.206
	KG-Mixup	0.308	0.133	0.420	0.325	0.145	0.446	0.136	0.037	0.175	0.192	0.107	0.210
	Booster	0.323	0.176	0.417	0.341	0.223	0.450	0.142	0.051	0.182	0.199	0.112	0.219
		Improve: 8.7%	P-value: 0.0114		Improve: 7.9%	P-value: 0.0101		Improve: 5.9%	P-value: 0.0225		Improve: 4.1%	P-value: 0.0217	
DE	Without DA	0.501	0.392	0.569	0.484	0.366	0.546	0.119	0.084	0.117	0.212	0.123	0.242
	MeTA	0.496	0.388	0.565	0.486	0.367	0.544	0.112	0.078	0.113	0.209	0.119	0.246
	DeMix	0.508	0.397	0.573	0.491	0.370	0.545	0.116	0.081	0.118	0.214	0.124	0.246
	NSCaching	0.503	0.394	0.570	0.482	0.365	0.541	0.115	0.080	0.116	0.217	0.125	0.248
	KG-Mixup	0.507	0.398	0.565	0.492	0.372	0.545	0.117	0.082	0.115	0.215	0.122	0.244
	Booster	0.521	0.410	0.578	0.510	0.388	0.548	0.124	0.086	0.118	0.221	0.126	0.252
		Improve: 3.9%	P-value: 0.0170		Improve: 3.5%	P-value: 0.0217		Improve: 4.2%	P-value: 0.0233		Improve: 4.2%	P-value: 0.0213	
TA	Without DA	0.409	0.295	0.466	0.492	0.376	0.544	0.110	0.072	0.108	0.188	0.109	0.210
	MeTA	0.405	0.293	0.460	0.493	0.377	0.542	0.112	0.078	0.104	0.186	0.107	0.208
	DeMix	0.411	0.292	0.473	0.498	0.380	0.545	0.106	0.071	0.103	0.184	0.106	0.210
	NSCaching	0.401	0.289	0.460	0.493	0.375	0.550	0.110	0.077	0.112	0.180	0.103	0.211
	KG-Mixup	0.412	0.290	0.475	0.502	0.381	0.544	0.113	0.075	0.110	0.191	0.110	0.210
	Booster	0.421	0.298	0.484	0.513	0.387	0.566	0.123	0.081	0.115	0.205	0.113	0.214
		Improve: 2.9%	P-value: 0.0156		Improve: 4.2%	P-value: 0.0139		Improve: 6.9%	P-value: 0.0218		Improve: 3.5%	P-value: 0.0185	
TEMP	Without DA	0.601	0.478	0.681	0.680	0.553	0.769	0.186	0.126	0.189	0.330	0.227	0.359
	MeTA	0.602	0.479	0.682	0.676	0.548	0.766	0.184	0.125	0.184	0.327	0.225	0.358
	DeMix	0.606	0.479	0.684	0.682	0.555	0.769	0.188	0.124	0.189	0.331	0.229	0.360
	NSCaching	0.598	0.476	0.677	0.678	0.550	0.764	0.180	0.121	0.187	0.325	0.220	0.356
	KG-Mixup	0.603	0.480	0.676	0.684	0.552	0.770	0.186	0.124	0.190	0.332	0.228	0.360
	Booster	0.623	0.485	0.690	0.697	0.559	0.779	0.194	0.130	0.195	0.340	0.237	0.362
		Improve: 3.6%	P-value: 0.0151		Improve: 2.5%	P-value: 0.0219		Improve: 4.3%	P-value: 0.0197		Improve: 3.3%	P-value: 0.0189	
TNT	Without DA	0.614	0.532	0.656	0.658	0.588	0.712	0.185	0.127	0.183	0.331	0.233	0.357
	MeTA	0.608	0.529	0.649	0.650	0.582	0.706	0.183	0.127	0.175	0.332	0.234	0.355
	DeMix	0.615	0.530	0.660	0.661	0.590	0.714	0.188	0.129	0.185	0.331	0.231	0.360
	NSCaching	0.605	0.526	0.649	0.652	0.584	0.709	0.180	0.123	0.176	0.327	0.228	0.355
	KG-Mixup	0.619	0.537	0.661	0.663	0.591	0.710	0.187	0.126	0.188	0.335	0.234	0.359
	Booster	0.636	0.557	0.678	0.679	0.602	0.728	0.195	0.131	0.201	0.342	0.239	0.367
		Improve: 3.5%	P-value: 0.0145		Improve: 3.2%	P-value: 0.0123		Improve: 5.4%	P-value: 0.0119		Improve: 3.3%	P-value: 0.0168	

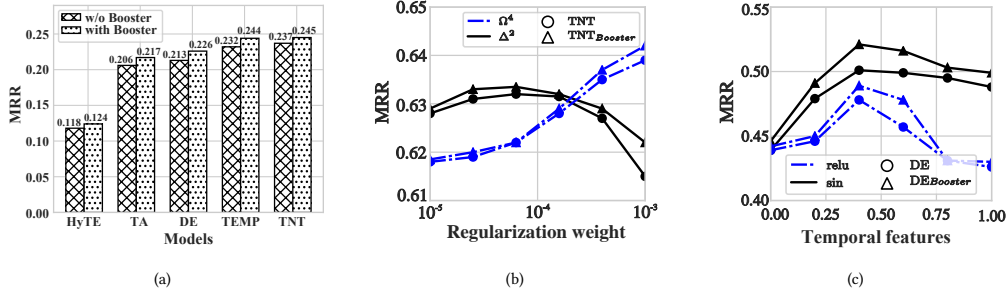


Figure 6: (a) Performance of different methods on the GDELDT dataset. (b) Performance improvements of *Booster* with varying hyper-parameters of the TNT model on the ICEWS 14 dataset. (c) Performance improvements of *Booster* with varying hyper-parameters of the DE model on the ICEWS 14 dataset.

improvement for most backbone models. Its improvement outperforms the powerful knowledge graph data augmentation strategies such as KG-Mixup and NSCaching, highlighting its effectiveness. One interesting observation is that some previous data augmentation strategies may even result in performance degradation such as MeTA and NSCaching. This is because they fail to fully consider TKGs’ complex semantic patterns and temporal relevance when filtering false negatives and generating new samples, and

thus bring noise to the TKGC models. (3) *Booster* shows performance improvements on all of the datasets, which demonstrates that it can adaptively handle heterogeneous temporal knowledge from different fields. We notice that the performance gains for a model may be different across datasets. The average improvement of different models on YAGO 11k is 3.9%, while on Wikidata 12k is 2.4%. This is because the sparsity of datasets can affect the performance gains. As shown in Figure 6(a), results on the GDELDT

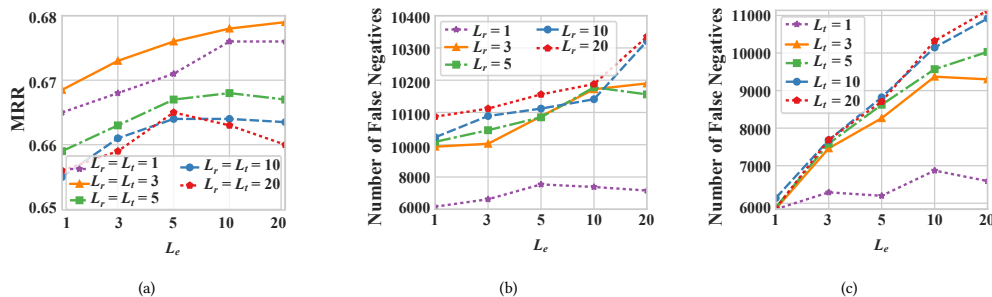


Figure 7: (a) Performance of $TNT_{Booster}$ with varying hyper-parameters on the ICEWS 05-15 dataset. (b) The number of identified false negatives with different L_e and L_r . (c) The number of identified false negatives with different L_e and L_t .

Table 3: Results of ablation study.

Dataset	ICEWS 14		Wikidata 12k	
	Hit@1	Hit@10	Hit@1	Hit@10
Variants				
w/o identified false negatives	0.545	0.774	0.334	0.541
w/o identified hard negatives	0.544	0.772	0.332	0.538
w/o model-specific hard samples	0.544	0.772	0.332	0.538
w/o entity scores	0.548	0.775	0.330	0.539
w/o relation scores	0.543	0.771	0.329	0.537
w/o smooth labels	0.533	0.768	0.331	0.537
w/o smooth labels + entity scores	0.523	0.760	0.324	0.534
w/o smooth labels + relation scores	0.521	0.757	0.322	0.530
$TNT_{Booster}$	0.557	0.781	0.342	0.547

Table 4: Performance comparison of variants.

Dataset	ICEWS 05-15		Wikidata 12k	
	Hit@1	Hit@10	Hit@1	Hit@10
Variants				
Identifying with DE	0.595	0.814	0.234	0.548
Identifying with TEMP	0.596	0.816	0.235	0.545
Self-training	0.582	0.791	0.230	0.539
Neighbor filtering	0.587	0.797	0.230	0.540
Recent active filtering	0.581	0.790	0.228	0.538
$TNT_{Booster}$	0.602	0.823	0.239	0.547

dataset verifies *Booster* can also achieve performance improvement on large graphs.

Hyper-parameter sensitivity. In Figure 6(b) and (c), Ω^4 and Δ^2 are hyper-parameters of TNT and DE. *sin* and *relu* are two nonlinear functions, and temporal features mean the percentage of time-sensitive representations. We can see that *Booster* can achieve improvement with different hyper-parameters of the original model. Figure 7(a) shows how the hyper-parameters of *Booster* affect its effectiveness. We can see that when L_e increases, *MRR* keeps increasing at first because the larger L_e helps to achieve more accurate scoring of facts. However, *MRR* drops when L_t and L_r are large. This is because the large L_t and L_r will extensively increase the number of filtered potential false negatives and thus bring more noise. Finally, Figure 7(b) and (c) show how the number of identified real false negatives changes with hyper-parameters. We can see that when L_r and L_t are large, the number of identified real false negatives increases significantly, but when $L_r = L_t = 1$, its number gradually decreases when L_e increases, which meets our conjecture that large L_t and L_r will bring more noise.

5.2 Effect of Each Component (RQ2)

Ablation study. Table 3 shows the ablation study results of *Booster*. we can see that including identified false negatives, hard negatives, and model-specific challenging samples during fine-tuning all contribute to performance. Removing the smooth label may cause performance degradation since the false negatives with low confidence will mislead the model during fine-tuning. Only removing entity scores or relation scores leads to small degradation, which also demonstrates the effectiveness of the smooth label in handling noises brought by false negative identification. However, when the

smooth label is removed, removing scores will largely damage the performance, which shows their benefit for accurate identification. We further show the sensitivity of model performance to the identified false negatives in Figure 8(a), where the variant without smooth label gets worse and more fluctuated performance. In Figure 8(b), we can see that fine-tuning the model is necessary for performance improvement. This has two reasons: 1) The pre-training is only based on a partial structure of the original graph, so it cannot accurately express the semantics of TKGs. 2) The fine-tuning samples are refined with various pattern-aware heuristics and thus enhance the model’s generalization ability to various TKG patterns. Moreover, the identified false negatives can enrich the sparse graph structure, and thus improve the performance for long-tail entities and timestamps.

Comparison with variants. Table 4 shows the performance of the variants of *Booster*. To verify the effectiveness of the hierarchical scoring algorithm, we replace it with the pre-trained DE and TEMP models to identify real false negatives. We can see that they fail to outperform our original framework. Moreover, as shown in Figure 8(c) and (d), retraining these models is time-consuming. The observations show the superiority of our proposed scoring algorithm. Furthermore, we directly employ self-training on the TNT model. We can see that the performance degrades significantly, which shows the necessity of considering model preferences. Finally, to verify the effectiveness of the filtering strategies, we compare our strategy with widely used false negative filtering strategies. Either selecting neighbor entities with sparse local structures or selecting the most recent active entities fail to achieve competitive performance to $TNT_{Booster}$.

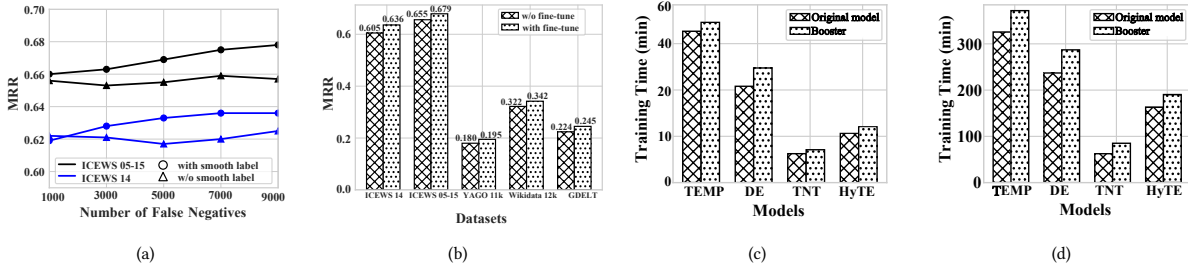


Figure 8: (a) The sensitivity of model performance to the identified false negatives. (b) Performance of the TNT model with and without fine-tuning. (c) The training time of different models on the ICEWS 14 dataset. (d) The training time of different models on the ICEWS 05-15 dataset.

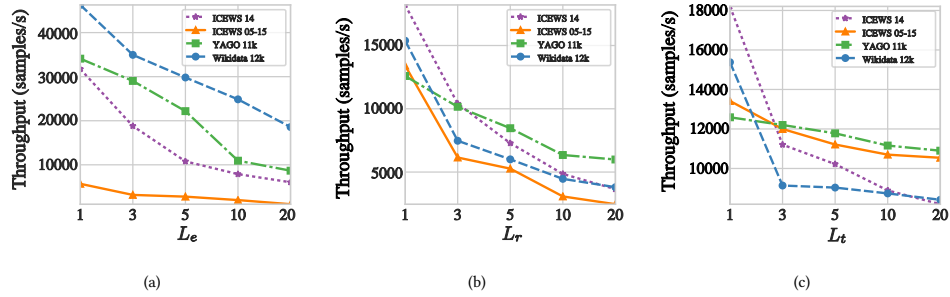


Figure 9: (a) Throughput of the Booster framework for processing different datasets with varying L_e . (b) Throughput of the Booster framework for processing different datasets with varying L_r . (c) Throughput of the Booster framework for processing different datasets with varying L_t .

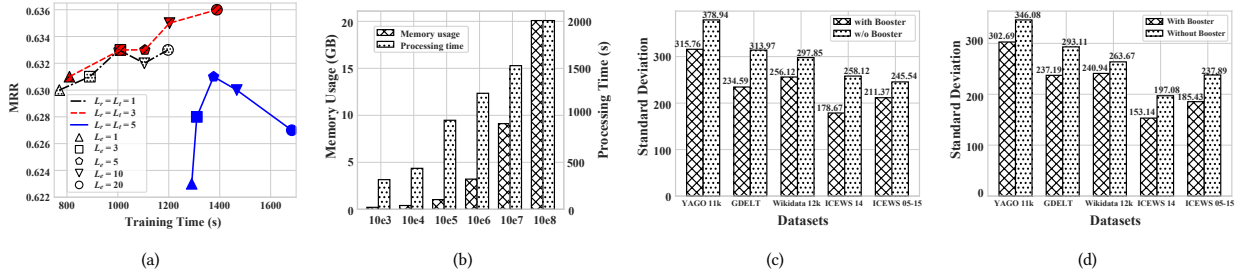


Figure 10: (a) MRR w.r.t. training time on the ICEWS 14 dataset. (b) Scalability of our proposed algorithm. (c) MRR variance on timestamps obtained by the TEMP model. (d) MRR variance on timestamps obtained by the TNT model.

5.3 Efficiency (RQ3)

Comparison with baselines. Figure 8(c) and (d) show the time consumption of baseline models when trained with the *Booster* framework. We can see that the training time is only increased by 1/10 and 1/5 for the TNT and TEMP models on the Wikidata 12k dataset. This is because they are not required to perform negative sampling during training and thus the additional time consumption only comes from the filtering and scoring. HyTE and DE require negative sampling. However, since the size of the hard negatives only increases sub-linearly with the size of the input TKG, the

additional time consumption of negative sampling does not increase significantly for large TKG (i.e., ICEWS 05-15). This demonstrates that *Booster* can improve the performance of existing TKGC models with an acceptable time consumption.

Throughput w.r.t. hyper-parameters. Figure 9 shows the throughput of filtering strategies and the hierarchical scoring algorithm with varying hyper-parameters. First, our proposed strategies achieve high throughput to all the hyper-parameters. The average processing time is nearly 0.5 ms per sample. Second, the throughput of our proposed strategies decreases sub-linearly when the span of

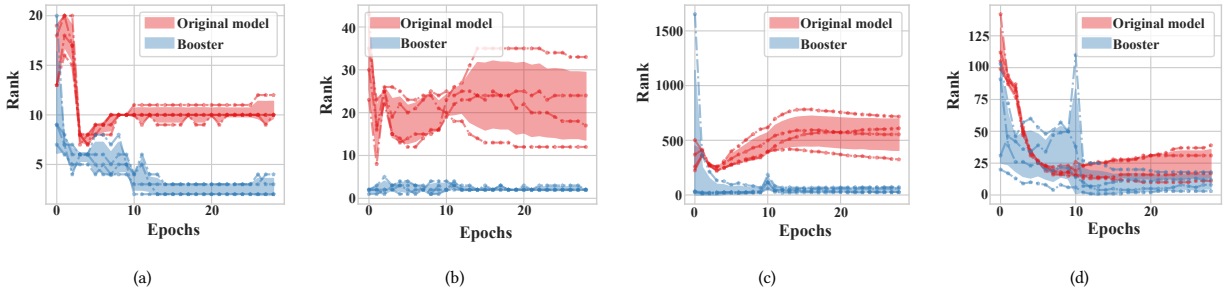


Figure 11: Change of *rank* of four test samples that are hard to be optimized by the TEMP model.

Table 5: Performance comparison on the ICEWS 14 dataset with different sparsities of timestamps and entities.

Models	HyTE	HyTE _{Booster}	TA	TA _{Booster}	TNT	TNT _{Booster}	
	MRR	MRR	MRR	MRR	MRR	MRR	
Time	Scope						
	[0:100]	0.255	0.291	0.421	0.447	0.598	0.621
	[100:250]	0.276	0.315	0.388	0.398	0.601	0.602
	[300:]	0.306	0.309	0.387	0.388	0.623	0.640
Entity	[0:10]	0.149	0.198	0.324	0.361	0.403	0.421
	[10:50]	0.287	0.306	0.378	0.383	0.585	0.598
	[100:]	0.343	0.357	0.411	0.428	0.634	0.639

the time window increases. This is because of the locality of TKGs that facts are mostly short-term related. Our strategies meet this property and thus can effectively filter out useless samples.

Tradeoff between MRR and training time. We conduct experiments to investigate the tradeoff between *MRR* and training time. Specifically, we set L_r and L_t as 1, 3, and 5. By varying L_e , we report the tradeoff between *MRR* and training time in Figure 10(a). We observe that when L_r and L_t are small, the *MRR* result increases as the training time increases. When $L_r = L_t = 5$ and L_e reaches 10, the training time keeps increasing but *MRR* degrades drastically.

Memory, CPU, and GPU usages. We use Psutil¹ to keep track of the memory and CPU usages and GPUUtil² to collect the GPU usage. The maximum memory usage of *Booster* is 14.51 GB. The total CPU utilization is 425% (the CPU has 10 cores and full CPU utilization is 1000%). The GPU utilization rate is 34%. As shown in Figure 10(b), the memory usage and processing time of our algorithm increase sub-linearly with increasing input graph size.

5.4 Balance and Stability (RQ4)

Balance. We analyze the performance improvement of *Booster* for samples with varying sparsity in Table 5. We first split the test samples based on the scope of their time sparsity (number of facts in each timestamp) and entity sparsity (number of interacted entities), and calculate the average *MRR* of samples in each scope. We can see that *Booster* can achieve performance improvement for samples with different sparsities. In particular, the improvement is larger for sparser samples, e.g., for samples with the number of interacted entities in the scope of [0:10], *Booster* achieves 11.7% improvement for TA, larger than 4.1% improvement for samples with the number of interacted entities in the scope of [100:]. This observation shows that *Booster* can effectively enrich the sparse

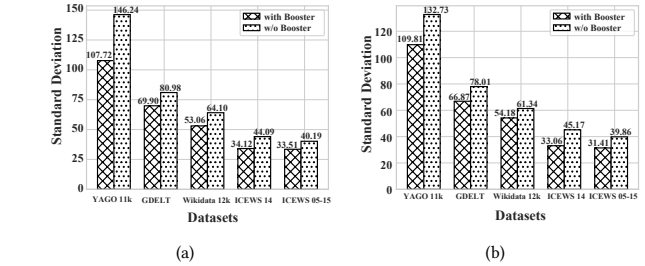


Figure 12: (a) Statistical study on the variance reduction of the TEMP model. (b) Statistical study on the variance reduction of the TNT model.

graph structures and thus achieve more balanced performance across timestamps and entities. As shown in Figure 10(c) and (d), we provide the standard deviation of the average *rank* metric among timestamps. We can see that by applying the *Booster* framework, baseline models can achieve lower standard deviations on different datasets, which also verifies the effectiveness of our framework in reducing the performance imbalance across timestamps.

Stability. To verify the effectiveness of *Booster* on stabilizing the performance, we randomly select four test samples whose performance results gradually get worse during training, and then we show the change of their *rank* metrics to training epochs on the TEMP model. As illustrated in Figure 11, all of these samples achieve better performance with a smaller fluctuation range when trained by the *Booster* framework. This is because *Booster* can alleviate the misleading of model preferences and avoid false negatives. In Figure 12, we show the standard deviations of *rank* of four independent training procedures. We can see that for all datasets, *Booster* can help different baseline models to get smaller standard deviations, which verifies its effectiveness in stabilizing performance.

6 CONCLUSION

In this paper, we make the first attempt to tackle the imbalanced data and model preference issues for temporal knowledge graph completion. We experimentally demonstrate existing methods' limitations, and then propose the first pattern-aware data augmentation framework tailored to TKGs to mitigate the impact of imbalanced

¹<https://pypi.org/project/psutil/>
²<https://pypi.org/project/GPUUtil/>

data and model preferences. Extensive experiments on five datasets demonstrate that *Booster* can help existing models achieve higher performance with better balance. For our future work, one promising direction is to study the robustness of existing TKG completion methods.

REFERENCES

- [1] Antoine Bordes, Nicolas Usunier, Alberto García-Durán, Jason Weston, and Oksana Yakhnenko. 2013. Translating Embeddings for Modeling Multi-relational Data. In *NIPS*. 2787–2795.
- [2] Elizabeth Boschee, Jennifer Lautenschlager, Sean O’Brien, Steve Shellman, James Starz, and Michael Ward. 2015. *ICEWS Coded Event Data*. Harvard Dataverse.
- [3] Heng Chang, Jie Cai, and Jia Li. 2023. Knowledge Graph Completion with Counterfactual Augmentation. In *The Web Conference*. 2611–2620.
- [4] Wei Chen, Huaiyu Wan, Yuting Wu, Shuyuan Zhao, Jiayaqi Cheng, Yuxin Li, and Youfang Lin. 2024. Local-Global History-Aware Contrastive Learning for Temporal Knowledge Graph Reasoning. In *ICDE*. 733–746.
- [5] Xiangnan Chen, Wen Zhang, Zhen Yao, Mingyang Chen, and Siliang Tang. 2023. Negative Sampling with Adaptive Denoising Mixup for Knowledge Graph Embedding. In *ISWC*. 253–270.
- [6] Jinhao Cui, Heyan Chai, Xu Yang, Ye Ding, Binxing Fang, and Qing Liao. 2024. SGCL: Semantic-aware Graph Contrastive Learning with Lipschitz Graph Augmentation. In *ICDE*. 3028–3041.
- [7] Shib Sankar Dasgupta, Swayambhu Nath Ray, and Partha P. Talukdar. 2018. HyTE: Hyperplane-based Temporally aware Knowledge Graph Embedding. In *EMNLP*. 2001–2011.
- [8] Kaize Ding, Zhe Xu, Hanghang Tong, and Huan Liu. 2022. Data Augmentation for Deep Graph Learning: A Survey. *SIGKDD Explor.* 24, 2 (2022), 61–77.
- [9] Fredo Erxleben, Michael Günther, Markus Kröttsch, Julian Mendez, and Denny Vrandečić. 2014. Introducing Wikidata to the Linked Data Web. In *ISWC*. 50–65.
- [10] Alberto García-Durán, Sebastijan Dumancic, and Mathias Niepert. 2018. Learning Sequence Encoders for Temporal Knowledge Graph Completion. In *EMNLP*. 4816–4821.
- [11] Justin Gilmer, Samuel S. Schoenholz, Patrick F. Riley, Oriol Vinyals, and George E. Dahl. 2017. Neural Message Passing for Quantum Chemistry. In *ICML*. 1263–1272.
- [12] Rishab Goel, Seyed Mehran Kazemi, Marcus A. Brubaker, and Pascal Poupart. 2020. Diachronic Embedding for Temporal Knowledge Graph Completion. In *AAAI*. 3988–3995.
- [13] Pankaj Gupta, Venu Satuluri, Ajeet Grewal, Siva Gurumurthy, Volodymyr Zhabuiuk, Quannan Li, and Jimmy Lin. 2014. Real-Time Twitter Recommendation: Online Motif Detection in Large Dynamic Graphs. *Proc. VLDB Endow.* 7, 13 (2014), 1379–1380.
- [14] Xiaotian Han, Zhimeng Jiang, Ninghao Liu, and Xia Hu. 2022. G-Mixup: Graph Data Augmentation for Graph Classification. In *ICML*, Vol. 162. 8230–8248.
- [15] Zhen Han, Peng Chen, Yunpu Ma, and Volker Tresp. 2021. Explainable Subgraph Reasoning for Forecasting on Temporal Knowledge Graphs. In *ICLR*.
- [16] Prachi Jain, Sushant Rath, Mausam, and Soumen Chakrabarti. 2020. Temporal Knowledge Base Completion: New Algorithms and Evaluation Protocols. In *EMNLP*. 3733–3747.
- [17] Mingxuan Ju, Tong Zhao, Wenhao Yu, Neil Shah, and Yanfang Ye. 2023. Graph-Patcher: Mitigating Degree Bias for Graph Neural Networks via Test-time Augmentation. In *NeurIPS*.
- [18] Hidetaka Kamigaito and Katsuhiko Hayashi. 2022. Comprehensive Analysis of Negative Sampling in Knowledge Graph Representation Learning. In *ICML*, Vol. 162. 10661–10675.
- [19] Timothée Lacroix, Guillaume Obozinski, and Nicolas Usunier. 2020. Tensor Decompositions for Temporal Knowledge Base Completion. In *ICLR*.
- [20] Kalev Leetaru and Philip A. Schrodtt. 2013. Global Database of Events, Language and Tone. In *ISA*.
- [21] Zixuan Li, Xiaolong Jin, Wei Li, Saiping Guan, Jiafeng Guo, Huawei Shen, Yuanzhuo Wang, and Xueqi Cheng. 2021. Temporal Knowledge Graph Reasoning Based on Evolutionary Representation Learning. In *SIGIR*. 408–417.
- [22] Hongrui Liu, Binbin Hu, Xiao Wang, Chuan Shi, Zhiqiang Zhang, and Jun Zhou. 2022. Confidence May Cheat: Self-Training on Graph Neural Networks under Distribution Shift. In *The Web Conference*. 1248–1258.
- [23] Bin Lu, Ze Zhao, Xiaoying Gan, Shiyu Liang, Luoyi Fu, Xinbing Wang, and Chenghu Zhou. 2024. Graph Out-of-Distribution Generalization With Controllable Data Augmentation. *IEEE Trans. Knowl. Data Eng.* 36, 11 (2024), 6317–6329.
- [24] A. Agnes Lydia and F. Sagayaraj Francis. 2019. Adagrad - An optimizer for stochastic gradient descent. *Int. J. Inf. Comput. Sci.* 6, 5 (2019), 566–568.
- [25] Tiroshan Madushanka and Ryutarō Ichise. 2024. Negative Sampling in Knowledge Graph Representation Learning: A Review. *CoRR abs/2402.19195* (2024).
- [26] Saurav Manchanda. 2023. Metapath-Guided Data-Augmentation For Knowledge Graphs. In *CIKM*. 4175–4179.
- [27] Zara Nasar, Syed Waqar Jaffry, and Muhammad Kamran Malik. 2022. Named Entity Recognition and Relation Extraction: State-of-the-Art. *ACM Comput. Surv.* 54, 1 (2022), 20:1–20:39.
- [28] Harry Shomer, Wei Jin, Wentao Wang, and Jiliang Tang. 2023. Toward Degree Bias in Embedding-Based Knowledge Graph Completion. In *The Web Conference*. 705–715.
- [29] Fabian M. Suchanek, Gjergji Kasneci, and Gerhard Weikum. 2007. Yago: a core of semantic knowledge. In *WWW*. 697–706.
- [30] Yongduo Sui, Qitian Wu, Jiancan Wu, Qing Cui, Longfei Li, Jun Zhou, Xiang Wang, and Xiangnan He. 2023. Unleashing the Power of Graph Data Augmentation on Covariate Distribution Shift. In *NeurIPS*.
- [31] Jizhi Tang, Yansong Feng, and Dongyan Zhao. 2019. Learning to Update Knowledge Graphs by Reading News. In *EMNLP-IJCNLP*. 2632–2641.
- [32] Xing Tang, Ling Chen, Hongyu Shi, and Dandan Liu. 2024. DHyper: A Recurrent Dual Hypergraph Neural Network for Event Prediction in Temporal Knowledge Graphs. *ACM Trans. Inf. Syst.* 42, 5 (2024), 129:1–129:23.
- [33] Xianfeng Tang, Huaxiu Yao, Yiwei Sun, Yiqi Wang, Jiliang Tang, Charu C. Aggarwal, Prasenjit Mitra, and Suhang Wang. 2020. Investigating and Mitigating Degree-Related Biases in Graph Convolutional Networks. In *CIKM*. 1435–1444.
- [34] Zhenwei Tang, Shichao Pei, Zhao Zhang, Yongchun Zhu, Fuzhen Zhuang, Robert Hoehndorf, and Xiangliang Zhang. 2022. Positive-Unlabeled Learning with Adversarial Data Augmentation for Knowledge Graph Completion. In *IJCAI*. 2248–2254.
- [35] Yuxing Tian, Aiwen Jiang, Qi Huang, Jian Guo, and Yiyan Qi. 2024. Latent Diffusion-based Data Augmentation for Continuous-Time Dynamic Graph Model. In *SIGKDD*. 2900–2911.
- [36] Jiapu Wang, Boyue Wang, Junbin Gao, Xiaoyan Li, Yongli Hu, and Baocai Yin. 2024. QDN: A Quadruplet Distributor Network for Temporal Knowledge Graph Completion. *IEEE Trans. Neural Networks Learn. Syst.* 35, 10 (2024), 14018–14030.
- [37] Jiapu Wang, Boyue Wang, Junbin Gao, Shirui Pan, Tengfei Liu, Baocai Yin, and Wen Gao. 2024. MADE: Multicurvature Adaptive Embedding for Temporal Knowledge Graph Completion. *IEEE Trans. Cybern.* 54, 10 (2024), 5818–5831.
- [38] Jiapu Wang, Boyue Wang, Meikang Qiu, Shirui Pan, Bo Xiong, Heng Liu, Linhao Luo, Tengfei Liu, Yongli Hu, Baocai Yin, and Wen Gao. 2023. A Survey on Temporal Knowledge Graph Completion: Taxonomy, Progress, and Prospects. *CoRR abs/2308.02457* (2023).
- [39] Yiwei Wang, Yujun Cai, Yuxuan Liang, Henghui Ding, Changhu Wang, Siddharth Bhatia, and Bryan Hooi. 2021. Adaptive Data Augmentation on Temporal Graphs. In *NeurIPS*. 1440–1452.
- [40] Jiapeng Wu, Meng Cao, Jackie Chi Kit Cheung, and William L. Hamilton. 2020. TeMP: Temporal Message Passing for Temporal Knowledge Graph Completion. In *EMNLP*. 5730–5746.
- [41] Yaochen Xie, Zhao Xu, Jingtun Zhang, Zhengyang Wang, and Shuiwang Ji. 2023. Self-Supervised Learning of Graph Neural Networks: A Unified Review. *IEEE Trans. Pattern Anal. Mach. Intell.* 45, 2 (2023), 2412–2429.
- [42] Hao Xin and Lei Chen. 2024. KartGPS: Knowledge Base Update with Temporal Graph Pattern-based Semantic Rules. In *ICDE*. 5075–5087.
- [43] Siheng Xiong, Yuan Yang, Faramarz Fekri, and James Clayton Kerce. 2023. TILP: Differentiable Learning of Temporal Logical Rules on Knowledge Graphs. In *ICLR*.
- [44] Chengjin Xu, Yung-Yu Chen, Mojtaba Nayyeri, and Jens Lehmann. 2021. Temporal Knowledge Graph Completion using a Linear Temporal Regularizer and Multivector Embeddings. In *NAACL-HLT*. 2569–2578.
- [45] Chenjin Xu, Mojtaba Nayyeri, Fouad Alkhoury, Hamed Shariat Yazdi, and Jens Lehmann. 2020. Temporal Knowledge Graph Completion Based on Time Series Gaussian Embedding. In *ISWC*. 654–671.
- [46] Chengjin Xu, Mojtaba Nayyeri, Fouad Alkhoury, Hamed Shariat Yazdi, and Jens Lehmann. 2020. TeRo: A Time-aware Knowledge Graph Embedding via Temporal Rotation. In *COLING*. 1583–1593.
- [47] Yi Xu, Junjie Ou, Hui Xu, and Luoyi Fu. 2023. Temporal Knowledge Graph Reasoning with Historical Contrastive Learning. In *AAAI*. 4765–4773.
- [48] Jinfa Yang, Xianghua Ying, Yongjie Shi, and Bowei Xing. 2024. Tensor decompositions for temporal knowledge graph completion with time perspective. *Expert Syst. Appl.* 237, Part A (2024), 121267.
- [49] Naimeng Yao, Qing Liu, Yi Yang, Weihua Li, and Quan Bai. 2023. Entity-Relation Distribution-Aware Negative Sampling for Knowledge Graph Embedding. In *ISWC*. 234–252.
- [50] Yuanzhou Yao, Zhao Zhang, Yongjun Xu, and Chao Li. 2022. Data Augmentation for Few-Shot Knowledge Graph Completion from Hierarchical Perspective. In *COLING*. 2494–2503.
- [51] Fu Zhang, Hongzhi Chen, Yuzhe Shi, Jingwei Cheng, and Jinghao Lin. 2024. Joint framework for tensor decomposition-based temporal knowledge graph completion. *Inf. Sci.* 654 (2024), 119853.
- [52] Mengqi Zhang, Yuwei Xia, Qiang Liu, Shu Wu, and Liang Wang. 2023. Learning Long- and Short-term Representations for Temporal Knowledge Graph Reasoning. In *The Web Conference*. 2412–2422.
- [53] Qianru Zhang, Lianghao Xia, Xuheng Cai, Siu-Ming Yiu, Chao Huang, and Christian S. Jensen. 2024. Graph Augmentation for Recommendation. In *ICDE*.

- 557–569.
- [54] Shuaicheng Zhang, Yada Zhu, and Dawei Zhou. 2023. TGEitor: Task-Guided Graph Editing for Augmenting Temporal Financial Transaction Networks. In *ICAF*. 219–226.
- [55] Yongqi Zhang, Quanming Yao, and Lei Chen. 2021. Simple and automated negative sampling for knowledge graph embedding. *VLDB J.* 30, 2 (2021), 259–285.
- [56] Yuyue Zhao, Xiang Wang, Jiawei Chen, Yashen Wang, Wei Tang, Xiangnan He, and Haiyong Xie. 2023. Time-aware Path Reasoning on Knowledge Graph for Recommendation. *ACM Trans. Inf. Syst.* 41, 2 (2023), 26:1–26:26.
- [57] Xinyi Zhu, Liping Wang, Hao Xin, Xiaohan Wang, Zhifeng Jia, Jiyao Wang, Chunming Ma, and Yuxiang Zeng. 2023. T-FinKB: A Platform of Temporal Financial Knowledge Base Construction. In *ICDE*. 3671–3674.